

ISSN 1726-5479

SENSORS & TRANSDUCERS

3^{vol. 14-2}
Special
/12



Physical and Chemical Sensors & Wireless Sensor Networks

International Frequency Sensor Association Publishing



Editors-in-Chief: Sergey Y. Yurish, tel.: +34 93 413 7941, e-mail: editor@sensorsportal.com**Editors for Western Europe**Meijer, Gerard C.M., Delft University of Technology, The Netherlands
Ferrari, Vittorio, Università di Brescia, Italy**Editor for Eastern Europe**

Sachenko, Anatoly, Ternopil State Economic University, Ukraine

Editors for North AmericaDatskos, Panos G., Oak Ridge National Laboratory, USA
Fabien, J. Josse, Marquette University, USA
Katz, Evgeny, Clarkson University, USA**Editor South America**

Costa-Felix, Rodrigo, Inmetro, Brazil

Editor for Africa

Maki K.Habib, American University in Cairo, Egypt

Editor for Asia

Ohyama, Shinji, Tokyo Institute of Technology, Japan

Editor for Asia-Pacific

Mukhopadhyay, Subhas, Massey University, New Zealand

Editorial Advisory Board

- Abdul Rahim, Ruzairi**, Universiti Teknologi, Malaysia
Ahmad, Mohd Noor, Nothern University of Engineering, Malaysia
Annamalai, Karthikeyan, National Institute of Advanced Industrial Science and Technology, Japan
Arcega, Francisco, University of Zaragoza, Spain
Arguel, Philippe, CNRS, France
Ahn, Jae-Pyoung, Korea Institute of Science and Technology, Korea
Arndt, Michael, Robert Bosch GmbH, Germany
Ascoli, Giorgio, George Mason University, USA
Atalay, Selcuk, Inonu University, Turkey
Atghiaee, Ahmad, University of Tehran, Iran
Augutis, Vyantas, Kaunas University of Technology, Lithuania
Avachit, Patil Lalchand, North Maharashtra University, India
Ayesh, Aladdin, De Montfort University, UK
Azamimi, Azian binti Abdullah, Universiti Malaysia Perlis, Malaysia
Bahreyni, Behraad, University of Manitoba, Canada
Baliga, Shankar, B., General Monitors Transnational, USA
Baoxian, Ye, Zhengzhou University, China
Barford, Lee, Agilent Laboratories, USA
Barlingay, Ravindra, RF Arrays Systems, India
Basu, Sukumar, Jadavpur University, India
Beck, Stephen, University of Sheffield, UK
Ben Bouzid, Sihem, Institut National de Recherche Scientifique, Tunisia
Benachaiba, Chellali, Universitaire de Bechar, Algeria
Binnie, T. David, Napier University, UK
Bischoff, Gerlinde, Inst. Analytical Chemistry, Germany
Bodas, Dhananjay, IMTEK, Germany
Borges Carval, Nuno, Universidade de Aveiro, Portugal
Bouchikhi, Benachir, University Moulay Ismail, Morocco
Bousbia-Salah, Mounir, University of Annaba, Algeria
Bouvet, Marcel, CNRS – UPMC, France
Brudzewski, Kazimierz, Warsaw University of Technology, Poland
Cai, Chenxin, Nanjing Normal University, China
Cai, Qingyun, Hunan University, China
Calvo-Gallego, Jaime, Universidad de Salamanca, Spain
Campanella, Luigi, University La Sapienza, Italy
Carvalho, Vitor, Minho University, Portugal
Cecelja, Franjo, Brunel University, London, UK
Cerda Belmonte, Judith, Imperial College London, UK
Chakrabarty, Chandan Kumar, Universiti Tenaga Nasional, Malaysia
Chakravorty, Dipankar, Association for the Cultivation of Science, India
Changhai, Ru, Harbin Engineering University, China
Chaudhari, Gajanan, Shri Shivaji Science College, India
Chavali, Murthy, N.I. Center for Higher Education, (N.I. University), India
Chen, Jiming, Zhejiang University, China
Chen, Rongshun, National Tsing Hua University, Taiwan
Cheng, Kuo-Sheng, National Cheng Kung University, Taiwan
Chiang, Jeffrey (Cheng-Ta), Industrial Technol. Research Institute, Taiwan
Chiriac, Horia, National Institute of Research and Development, Romania
Chowdhuri, Arijit, University of Delhi, India
Chung, Wen-Yaw, Chung Yuan Christian University, Taiwan
Corres, Jesus, Universidad Publica de Navarra, Spain
Cortes, Camilo A., Universidad Nacional de Colombia, Colombia
Courtois, Christian, Universite de Valenciennes, France
Cusano, Andrea, University of Sannio, Italy
D'Amico, Arnaldo, Università di Tor Vergata, Italy
De Stefano, Luca, Institute for Microelectronics and Microsystem, Italy
Deshmukh, Kiran, Shri Shivaji Mahavidyalaya, Barshi, India
Dickert, Franz L., Vienna University, Austria
Dieguez, Angel, University of Barcelona, Spain
Dighavkar, C. G., M.G. Vidyamandir's L. V.H. College, India
Dimitropoulos, Panos, University of Thessaly, Greece
Ding, Jianning, Jiangsu Polytechnic University, China
Djordjevich, Alexandar, City University of Hong Kong, Hong Kong
Donato, Nicola, University of Messina, Italy
Donato, Patricio, Universidad de Mar del Plata, Argentina
Dong, Feng, Tianjin University, China
Drljaca, Predrag, Instersema Sensoric SA, Switzerland
Dubey, Venketesh, Bournemouth University, UK
Enderle, Stefan, Univ.of Ulm and KTB Mechatronics GmbH, Germany
Erdem, Gursan K. Arzum, Ege University, Turkey
Erkmen, Aydan M., Middle East Technical University, Turkey
Estelle, Patrice, Insa Rennes, France
Estrada, Horacio, University of North Carolina, USA
Faiz, Adil, INSA Lyon, France
Fericean, Sorin, Balluff GmbH, Germany
Fernandes, Joana M., University of Porto, Portugal
Francioso, Luca, CNR-IMM Institute for Microelectronics and Microsystems, Italy
Francis, Laurent, University Catholique de Louvain, Belgium
Fu, Weiling, South-Western Hospital, Chongqing, China
Gaura, Elena, Coventry University, UK
Geng, Yanfeng, China University of Petroleum, China
Gole, James, Georgia Institute of Technology, USA
Gong, Hao, National University of Singapore, Singapore
Gonzalez de la Rosa, Juan Jose, University of Cadiz, Spain
Granell, Annette, Goteborg University, Sweden
Graff, Mason, The University of Texas at Arlington, USA
Guan, Shan, Eastman Kodak, USA
Guillet, Bruno, University of Caen, France
Guo, Zhen, New Jersey Institute of Technology, USA
Gupta, Narendra Kumar, Napier University, UK
Hadjiloucas, Sillas, The University of Reading, UK
Haider, Mohammad R., Sonoma State University, USA
Hashsham, Syed, Michigan State University, USA
Hasni, Abdelhafid, Bechar University, Algeria
Hernandez, Alvaro, University of Alcalá, Spain
Hernandez, Wilmar, Universidad Politecnica de Madrid, Spain
Homentcovschi, Dorel, SUNY Binghamton, USA
Horstman, Tom, U.S. Automation Group, LLC, USA
Hsiai, Tzung (John), University of Southern California, USA
Huang, Jeng-Sheng, Chung Yuan Christian University, Taiwan
Huang, Star, National Tsing Hua University, Taiwan
Huang, Wei, PSG Design Center, USA
Hui, David, University of New Orleans, USA
Jaffrezic-Renault, Nicole, Ecole Centrale de Lyon, France
James, Daniel, Griffith University, Australia
Janting, Jakob, DELTA Danish Electronics, Denmark
Jiang, Liudi, University of Southampton, UK
Jiang, Wei, University of Virginia, USA
Jiao, Zheng, Shanghai University, China
John, Joachim, IMEC, Belgium
Kalach, Andrew, Voronezh Institute of Ministry of Interior, Russia
Kang, Moonho, Sunmoon University, Korea South
Kaniasus, Eugenijus, Vienna University of Technology, Austria
Katake, Anup, Texas A&M University, USA
Kausel, Wilfried, University of Music, Vienna, Austria
Kavasoglu, Nese, Mugla University, Turkey
Ke, Cathy, Tyndall National Institute, Ireland
Khelfaoui, Rachid, Université de Bechar, Algeria
Khan, Asif, Aligarh Muslim University, Aligarh, India
Kim, Min Young, Kyungpook National University, Korea South
Ko, Sang Choon, Electronics. and Telecom. Research Inst., Korea South
Kotulska, Malgorzata, Wroclaw University of Technology, Poland
Kockar, Hakan, Balikesir University, Turkey

Kong, Ing, RMIT University, Australia
Kratz, Henrik, Uppsala University, Sweden
Krishnamoorthy, Ganesh, University of Texas at Austin, USA
Kumar, Arun, University of Delaware, Newark, USA
Kumar, Subodh, National Physical Laboratory, India
Kung, Chih-Hsien, Chang-Jung Christian University, Taiwan
Lacnjevac, Caslav, University of Belgrade, Serbia
Lay-Ekuakille, Aime, University of Lecce, Italy
Lee, Jang Myung, Pusan National University, Korea South
Lee, Jun Su, Amkor Technology, Inc. South Korea
Lei, Hua, National Starch and Chemical Company, USA
Li, Fengyuan (Thomas), Purdue University, USA
Li, Genxi, Nanjing University, China
Li, Hui, Shanghai Jiaotong University, China
Li, Xian-Fang, Central South University, China
Li, Yuefa, Wayne State University, USA
Liang, Yuanchang, University of Washington, USA
Liawruangrath, Saisunee, Chiang Mai University, Thailand
Liew, Kim Meow, City University of Hong Kong, Hong Kong
Lin, Hermann, National Kaohsiung University, Taiwan
Lin, Paul, Cleveland State University, USA
Linderholm, Pontus, EPFL - Microsystems Laboratory, Switzerland
Liu, Aihua, University of Oklahoma, USA
Liu Changgeng, Louisiana State University, USA
Liu, Cheng-Hsien, National Tsing Hua University, Taiwan
Liu, Songqin, Southeast University, China
Lodeiro, Carlos, University of Vigo, Spain
Lorenzo, Maria Encarnacio, Universidad Autonoma de Madrid, Spain
Lukaszewicz, Jerzy Pawel, Nicholas Copernicus University, Poland
Ma, Zhanfang, Northeast Normal University, China
Majstorovic, Vidosav, University of Belgrade, Serbia
Malyshev, V.V., National Research Centre 'Kurchatov Institute', Russia
Marquez, Alfredo, Centro de Investigacion en Materiales Avanzados, Mexico
Matay, Ladislav, Slovak Academy of Sciences, Slovakia
Mathur, Prafull, National Physical Laboratory, India
Maurya, D.K., Institute of Materials Research and Engineering, Singapore
Mekid, Samir, University of Manchester, UK
Melnyk, Ivan, Photon Control Inc., Canada
Mendes, Paulo, University of Minho, Portugal
Mennell, Julie, Northumbria University, UK
Mi, Bin, Boston Scientific Corporation, USA
Minas, Graca, University of Minho, Portugal
Moghavvemi, Mahmoud, University of Malaya, Malaysia
Mohammadi, Mohammad-Reza, University of Cambridge, UK
Molina Flores, Esteban, Benemerita Universidad Autónoma de Puebla, Mexico
Moradi, Majid, University of Kerman, Iran
Morello, Rosario, University "Mediterranea" of Reggio Calabria, Italy
Mounir, Ben Ali, University of Sousse, Tunisia
Mrad, Nezih, Defence R&D, Canada
Mulla, Imtiaz Sirajuddin, National Chemical Laboratory, Pune, India
Nabok, Aleksey, Sheffield Hallam University, UK
Neelamegam, Periasamy, Sastra Deemed University, India
Neshkova, Milka, Bulgarian Academy of Sciences, Bulgaria
Oberhammer, Joachim, Royal Institute of Technology, Sweden
Ould Lahoucine, Cherif, University of Guelma, Algeria
Pamidighanta, Sayanu, Bharat Electronics Limited (BEL), India
Pan, Jisheng, Institute of Materials Research & Engineering, Singapore
Park, Joon-Shik, Korea Electronics Technology Institute, Korea South
Penza, Michele, ENEA C.R., Italy
Pereira, Jose Miguel, Instituto Politecnico de Seteбал, Portugal
Petsev, Dimiter, University of New Mexico, USA
Pogacnik, Lea, University of Ljubljana, Slovenia
Post, Michael, National Research Council, Canada
Prance, Robert, University of Sussex, UK
Prasad, Ambika, Gulbarga University, India
Prateepasen, Asa, Kingmoungut's University of Technology, Thailand
Pugno, Nicola M., Politecnico di Torino, Italy
Pullini, Daniele, Centro Ricerche FIAT, Italy
Pumera, Martin, National Institute for Materials Science, Japan
Radhakrishnan, S., National Chemical Laboratory, Pune, India
Rajanna, K., Indian Institute of Science, India
Ramadan, Qasem, Institute of Microelectronics, Singapore
Rao, Basuthkar, Tata Inst. of Fundamental Research, India
Raouf, Kosai, Joseph Fourier University of Grenoble, France
Rastogi Shiva, K., University of Idaho, USA
Reig, Candid, University of Valencia, Spain
Restivo, Maria Teresa, University of Porto, Portugal
Robert, Michel, University Henri Poincare, France
Rezazadeh, Ghader, Urmia University, Iran
Royo, Santiago, Universitat Politecnica de Catalunya, Spain
Rodriguez, Angel, Universidad Politecnica de Cataluna, Spain
Rothberg, Steve, Loughborough University, UK
Sadana, Ajit, University of Mississippi, USA
Sadeghian Marnani, Hamed, TU Delft, The Netherlands
Sapozhnikova, Ksenia, D.I.Mendeleyev Institute for Metrology, Russia
Sandacci, Serghei, Sensor Technology Ltd., UK
Saxena, Vibha, Bbhba Atomic Research Centre, Mumbai, India
Schneider, John K., Ultra-Scan Corporation, USA
Sengupta, Deepak, Advance Bio-Photonics, India
Seif, Selemeni, Alabama A & M University, USA
Seifter, Achim, Los Alamos National Laboratory, USA
Shah, Kriyang, La Trobe University, Australia
Sankarraaj, Anand, Detector Electronics Corp., USA
Silva Girao, Pedro, Technical University of Lisbon, Portugal
Singh, V. R., National Physical Laboratory, India
Slomovitz, Daniel, UTE, Uruguay
Smith, Martin, Open University, UK
Soleymanpour, Ahmad, Damghan Basic Science University, Iran
Somani, Prakash R., Centre for Materials for Electronics Technol., India
Sridharan, M., Sastra University, India
Srinivas, Talabattula, Indian Institute of Science, Bangalore, India
Srivastava, Arvind K., NanoSonix Inc., USA
Stefan-van Staden, Raluca-Ioana, University of Pretoria, South Africa
Stefanescu, Dan Mihai, Romanian Measurement Society, Romania
Sumriddetchka, Sarun, National Electronics and Computer Technology Center, Thailand
Sun, Chengliang, Polytechnic University, Hong-Kong
Sun, Dongming, Jilin University, China
Sun, Junhua, Beijing University of Aeronautics and Astronautics, China
Sun, Zhiqing, Central South University, China
Suri, C. Raman, Institute of Microbial Technology, India
Sysoev, Victor, Saratov State Technical University, Russia
Szewczyk, Roman, Industrial Research Inst. for Automation and Measurement, Poland
Tan, Ooi Kiang, Nanyang Technological University, Singapore
Tang, Dianping, Southwest University, China
Tang, Jaw-Luen, National Chung Cheng University, Taiwan
Teker, Kasif, Frostburg State University, USA
Thirunavukkarasu, I., Manipal University Karnataka, India
Thumavanam Pad, Kartik, Carnegie Mellon University, USA
Tian, Gui Yun, University of Newcastle, UK
Tsiantos, Vassilios, Technological Educational Institute of Kaval, Greece
Tsigara, Anna, National Hellenic Research Foundation, Greece
Twomey, Karen, University College Cork, Ireland
Valente, Antonio, University, Vila Real, - U.T.A.D., Portugal
Vanga, Raghav Rao, Summit Technology Services, Inc., USA
Vaseashta, Ashok, Marshall University, USA
Vazquez, Carmen, Carlos III University in Madrid, Spain
Vieira, Manuela, Instituto Superior de Engenharia de Lisboa, Portugal
Vigna, Benedetto, STMicroelectronics, Italy
Vrba, Radimir, Brno University of Technology, Czech Republic
Wandelt, Barbara, Technical University of Lodz, Poland
Wang, Jiangping, Xi'an Shiyou University, China
Wang, Kedong, Beihang University, China
Wang, Liang, Pacific Northwest National Laboratory, USA
Wang, Mi, University of Leeds, UK
Wang, Shinn-Fwu, Ching Yun University, Taiwan
Wang, Wei-Chih, University of Washington, USA
Wang, Wensheng, University of Pennsylvania, USA
Watson, Steven, Center for NanoSpace Technologies Inc., USA
Weiping, Yan, Dalian University of Technology, China
Wells, Stephen, Southern Company Services, USA
Wolkenberg, Andrzej, Institute of Electron Technology, Poland
Woods, R. Clive, Louisiana State University, USA
Wu, DerHo, National Pingtung Univ. of Science and Technology, Taiwan
Wu, Zhaoyang, Hunan University, China
Xiu Tao, Ge, Chuzhou University, China
Xu, Lisheng, The Chinese University of Hong Kong, Hong Kong
Xu, Sen, Drexel University, USA
Xu, Tao, University of California, Irvine, USA
Yang, Dongfang, National Research Council, Canada
Yang, Shuang-Hua, Loughborough University, UK
Yang, Wuqiang, The University of Manchester, UK
Yang, Xiaoling, University of Georgia, Athens, GA, USA
Yaping Dan, Harvard University, USA
Ymeti, Aurel, University of Twente, Netherland
Yong Zhao, Northeastern University, China
Yu, Haihu, Wuhan University of Technology, China
Yuan, Yong, Massey University, New Zealand
Yufera Garcia, Alberto, Seville University, Spain
Zakaria, Zulkarnay, University Malaysia Perlis, Malaysia
Zagnoni, Michele, University of Southampton, UK
Zamani, Cyrus, Universitat de Barcelona, Spain
Zeni, Luigi, Second University of Naples, Italy
Zhang, Minglong, Shanghai University, China
Zhang, Qintao, University of California at Berkeley, USA
Zhang, Weiping, Shanghai Jiao Tong University, China
Zhang, Wenming, Shanghai Jiao Tong University, China
Zhang, Xueji, World Precision Instruments, Inc., USA
Zhong, Haoxiang, Henan Normal University, China
Zhu, Qing, Fujifilm Dimatix, Inc., USA
Zorzano, Luis, Universidad de La Rioja, Spain
Zourob, Mohammed, University of Cambridge, UK

Contents

Volume 14-2
Special Issue
March 2012

www.sensorsportal.com

ISSN 1726-5479

Research Articles

Information Extraction from Wireless Sensor Networks: System and Approaches <i>Tariq Alsboui, Abdelrahman Abuarqoub, Mohammad Hammoudeh, Zuhair Bandar, Andy Nisbet...</i>	1
Assessment of Software Modeling Techniques for Wireless Sensor Networks: A Survey <i>John Khalil Jacoub, Ramiro Liscano, Jeremy S. Bradbury</i>	18
Effective Management and Energy Efficiency in Management of Very Large Scale Sensor Network <i>Moran Feldman, Sharoni Feldman</i>	47
Energy Efficient in-Sensor Data Cleaning for Mining Frequent Itemsets <i>Jacques M. Bahi, Abdallah Makhoul, Maguy Medlej</i>	64
IPv6 Routing Protocol for Low Power and Lossy Sensor Networks Simulation Studies <i>Leila Ben Saad, Cedric Chauvenet, Bernard Tourancheau</i>	79
Self-Powered Intelligent Sensor Node Concept for Monitoring of Road and Traffic Conditions <i>Sebastian Strache, Ralf Wunderlich and Stefan Heinen</i>	93
Variable Step Size LMS Algorithm for Data Prediction in Wireless Sensor Networks <i>Biljana Risteska Stojkoska, Dimitar Solev, Danco Davcev</i>	111
A Framework for Secure Data Delivery in Wireless Sensor Networks <i>Leonidas Perlepes, Alexandros Zaharis, George Stamoulis and Panagiotis Kikiras</i>	125
An Approach for Designing and Implementing Middleware in Wireless Sensor Networks <i>Ronald Beaubrun, Jhon-Fredy Llano-Ruiz, Alejandro Quintero</i>	150
Mobility Model for Self-Organizing and Cooperative MSN and MANET Systems <i>Andrzej Sikora and Ewa Niewiadomska-Szynkiewicz</i>	164
Evaluation of Hybrid Distributed Least Squares for Improved Localization via Algorithm Fusion in Wireless Sensor Networks <i>Ralf Behnke, Jakob Salzmann, Philipp Gorski, Dirk Timmermann</i>	179
An Effective Approach for Handling both Open and Closed Voids in Wireless Sensor Networks <i>Mohamed Aissani, Sofiane Bouznad, Abdelmalek Hariza and Salah-Eddine Allia</i>	196
Embedded Wireless System for Pedestrian Localization in Indoor Environments <i>Nicolas Fourty, Yoann Charlon, Eric Campo</i>	211
Neighbourtables – A Cross-layer Solution for Wireless CiNet Network Analysis and Diagnostics <i>Ismo Hakala and Timo Hongell</i>	228

A Column Generation based Heuristic to extend Lifetime in Wireless Sensor Network <i>Karine Deschinkel</i>	242
Adapting OLSR for WSNs (iOLSR) Using Locally Increasing Intervals <i>Erlend Larsen, Joakim Flathagen, Vinh Pham, Lars Landmark</i>	254
Risk Assessment along Supply Chain: A RFID and Wireless Sensor Network Integration Approach <i>Laurent Gomez, Maryline Laurent, Ethmane El Moustaine</i>	269
Structure Crack Identification Based on Surface-mounted Active Sensor Network with Time-Domain Feature Extraction and Neural Network <i>Chunling Du, Jianqiang Mou, L. Martua, Shudong Liu, Bingjin Chen, Jingliang Zhang, F. L. Lewis.</i>	283
Efficient Gatherings in Wireless Sensor Networks Using Distributed Computation of Connected Dominating Sets <i>Vincent Boudet, Sylvain Durand, László Gönczy, Jérôme Mathieu and Jérôme Palaysi</i>	297
Secure Packet Transfer in Wireless Sensor Networks <i>Yenumula B. Reddy</i>	308

Authors are encouraged to submit article in MS Word (doc) and Acrobat (pdf) formats by e-mail: editor@sensorsportal.com
Please visit journal's webpage with preparation instructions: <http://www.sensorsportal.com/HTML/DIGEST/Submission.htm>

International Frequency Sensor Association (IFSA).

IMAGE SENSORS 2012
TWO DAY INTERTECHPIRA CONFERENCE PLUS EXPERT PRE-CONFERENCE WORKSHOPS
FOCUS ON DIGITAL IMAGING

PRESENTATIONS FROM:

- SoftKinetic
- BBC
- NASA
- NHS
- Leica Geosystems
- Sony Ericsson
- OLYMPUS
- SIEMENS
- Panasonic Ideas for life
- raytrix
- BOSCH
- SAFRAN
- Leti
- SAFRAN
- caeleste
- PELCO
- SONY
- Aptina
- NMK

SUPPORTING PARTNERS:

- Plastic
- IFSA
- 3D Packaging
- imaging and machine vision
- Micronews
- cmva

REGISTER NOW → IMAGE-SENSORS.COM

OVERVIEW → WHY ATTEND → TUES 20 MAR → WED 21 MAR → THURS 22 MAR → VENUE →

IMAGE SENSORS 2012
20-22 March
Hotel Russell
London

The 6th International Conference on Sensor Technologies and Applications



SENSORCOMM 2012

19 - 24 August 2012 - Rome, Italy

Deadline for papers: 5 April 2012



Tracks: Architectures, protocols and algorithms of sensor networks - Energy, management and control of sensor networks - Resource allocation, services, QoS and fault tolerance in sensor networks - Performance, simulation and modelling of sensor networks - Security and monitoring of sensor networks - Sensor circuits and sensor devices - Radio issues in wireless sensor networks - Software, applications and programming of sensor networks - Data allocation and information in sensor networks - Deployments and implementations of sensor networks - Under water sensors and systems - Energy optimization in wireless sensor networks

<http://www.aria.org/conferences2012/SENSORCOMM12.html>

The 3rd International Conference on Sensor Device Technologies and Applications



SENSORDEVICES 2012

19 - 24 August 2012 - Rome, Italy

Deadline for papers: 5 April 2012



Tracks: Sensor devices - Ultrasonic and Piezosensors - Photonics - Infrared - Geosensors - Sensor device technologies - Sensors signal conditioning and interfacing circuits - Medical devices and sensors applications - Sensors domain-oriented devices, technologies, and applications - Sensor-based localization and tracking technologies

<http://www.aria.org/conferences2012/SENSORDEVICES12.html>

The 5th International Conference on Advances in Circuits, Electronics and Micro-electronics



CENICS 2012

19 - 24 August 2012 - Rome, Italy

Deadline for papers: 5 April 2012



Tracks: Semiconductors and applications - Design, models and languages - Signal processing circuits - Arithmetic computational circuits - Microelectronics - Electronics technologies - Special circuits - Consumer electronics - Application-oriented electronics

<http://www.aria.org/conferences2012/CENICS12.html>

Self-Powered Intelligent Sensor Node Concept for Monitoring of Road and Traffic Conditions

Sebastian Strache, Ralf Wunderlich and Stefan Heinen

Chair of Integrated Analog Circuits and RF Systems, RWTH Aachen University,
Templergraben 55, 52062, Germany
Tel.: +49 241-80 27746, fax +49 241-80 22199
E-mail: ias@rwth-aachen.de

Received: 15 November 2011 /Accepted: 20 December 2011 /Published: 12 March 2012

Abstract: A promising approach for future road construction is based on a surface, which is manufactured in a production plant and can be unrolled on a conventional basis. This paper deals with an idea of making the road “intelligent” by integrating a net of sensor nodes. Equipped with acceleration sensors these systems can detect the actual traffic situation. With the knowledge of the exact position and velocity of each car a driver assistance system is able to find the fastest route or provide exact and reliable warnings to prevent e.g. accidents at the end of traffic jams. This paper describes the main idea of a low cost, energy harvesting sensor node containing a MEMS accelerometer with a frontend, a processing unit, a photovoltaic energy harvesting power supply and a wireless communication link. Measurements show that the detection of passing vehicles using structure borne sound and MEMS accelerometers is feasible. Furthermore the described functionality can be integrated into a size of less than $2.45\text{ cm} \times 2.45\text{ cm} \times 1\text{ cm}$ and each sensor node can be operated stand alone. *Copyright © 2012 IFSA.*

Keywords: Road construction, Intelligent road, MEMS, Energy harvesting, Sensor node.

1. Introduction

The next step in road building is to introduce a high quality, centimeter thin top cover manufactured in production plants probably on the base of a synthetic material. Better noise reduction and lower rolling drag can be achieved, since a production in a plant is done under best conditions. The feasibility of a “rollable” road has been shown in [1, 2]. Conventional streets need a large amount of (oil based) bitumen, which is running out and therefore getting more and more expensive. In order to damp down

the cost increase the amount of bitumen needed has to be reduced by decreasing the thickness of the bitumen based top layer of the road or to find a low priced suitable alternative material.

The road systems of developed countries form the backbones of their economies. Intelligent traffic management systems increase the traffic capacity without building new roads. These systems need exact information about the traffic flow to avoid traffic jams and minimize the individual traveling times. The quality of traffic management heavily depends on good input data. Further, it is getting more and more challenging and expensive to enhance the safety with vehicle based systems. In the near future driving assistance systems will be upgraded to highly automated, nearly autonomous systems, which need more reliable data to process. Vehicle based sensor systems are not able to provide data off the required quality level for every situation as shown by [3]. In contrast to these vehicles based systems, this paper proposes an infrastructure that can be used for autonomous driving in the long run. Furthermore it can provide additional information about the road situation and conditions ahead for every individual vehicle, such as humidity, temperature and slickness which are unknown for vehicle based systems.

This paper subdivides into nine chapters. Section 2 presents the system concept of the “intelligent” road. In section 3, the body sound measurements conducted on a test track will be discussed. Then the sensor node itself will be shown in section 4. The power supply of the sensor is described in section 5, followed by the transmitter in section 6. Afterwards section 7 gives more details on the requirements for the accelerometer. The high resolution, low power accelerometer read out circuit is presented in section 8. Finally conclusions are drawn and an outlook is given in section 9.

2. System Concept

Fig. 1 shows a cross section of the car-pad road. The base layer can be build conventionally; the top layer is called car-pad (in analogy to carpet). The centimeter thin, high quality, industrially produced car-pad is unrolled and mounted onto the conventional base. Therefore, the time required for construction works is short. The industrial fabrication of the car-pad enables the integration of sensors inside the top layer of the road (colored dots in Fig. 1). Integrated wireless sensor nodes enable the detection of passing vehicles and measure different ambient road conditions, such as temperature or moisture. The cost of the sensor net is almost insignificant compared to present-day's overall road costs.

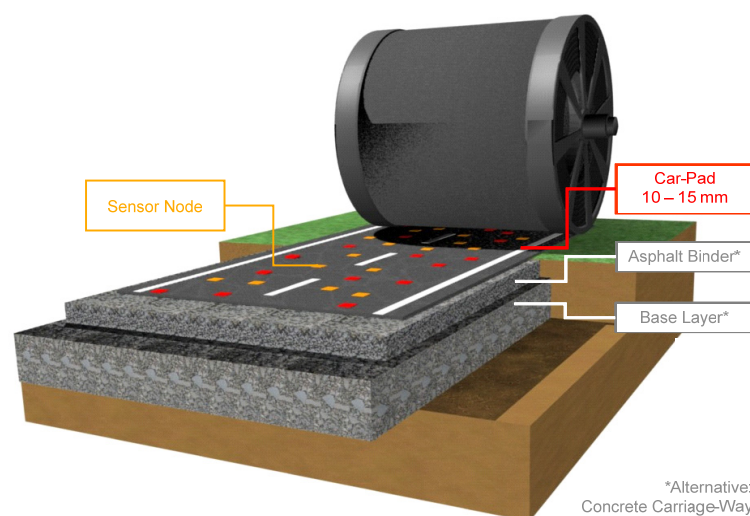


Fig. 1. Cross section car-pad [4].

The system concept and the needed infrastructure to utilize the information gained by the integrated sensor nodes are illustrated in Fig. 2. Vehicles moving on the car-pad generate structure-borne sound, which propagates through the top layer of the road and can be detected by an accelerometer. Accelerometers have very small dimensions, are cheap and can easily be integrated inside a sensor node. After preprocessing, the data is transmitted to small base stations mounted in beacons at the side of the road. These base stations combine the information of the different sensor nodes, generate a more global view of the traffic flow at this part of the road, and transmit this information to both, a central traffic management center and the passing cars.

Due to the high density of the sensor network not only the traffic flow, but also local security relevant events, like accidents or cars in blind spots, can be detected and road users can be warned. Since the information is determined by the infrastructure and not by a car based system, the system will even work, if most users are not equipped with a vehicle on-board unit. To benefit from these warning signals no special hardware is necessary. The on-board unit can e.g. be integrated into the navigation system.

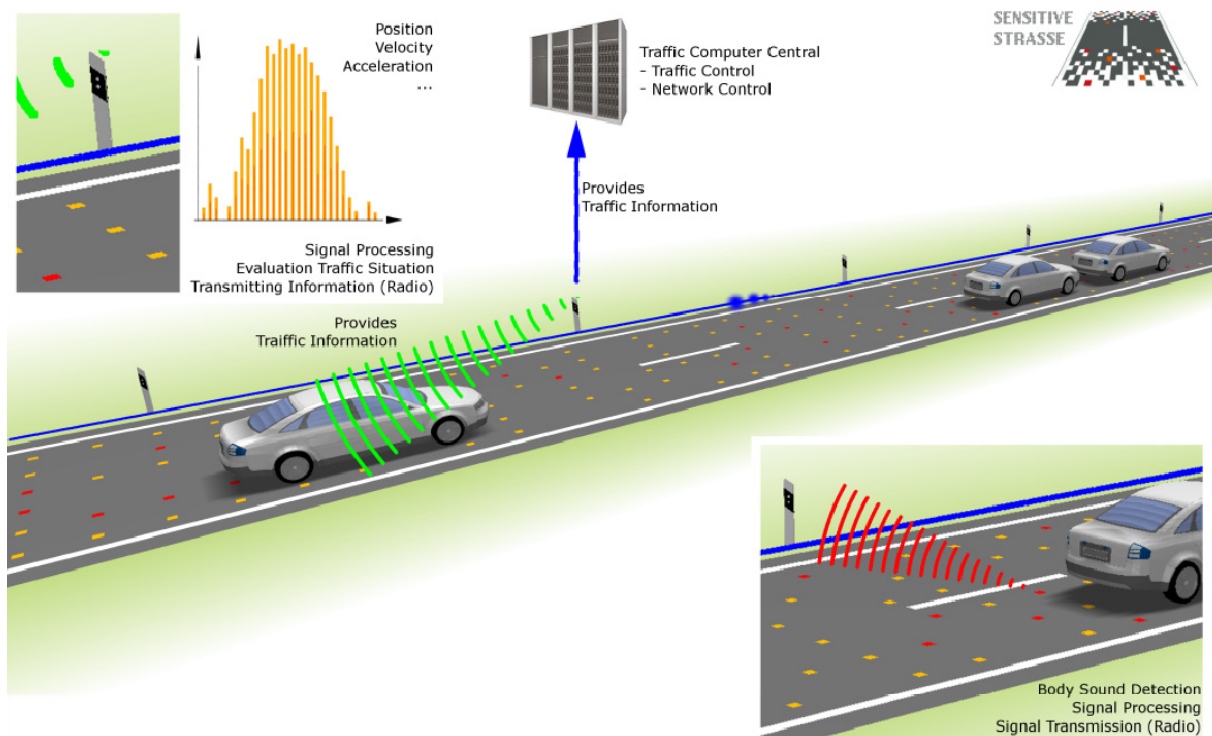


Fig. 2. Car-pad idea and infrastructure [4].

3. Measurements

To the best of the authors' knowledge, this is the first project, which proposes the use of structure-borne sound for vehicle detection. Since there was no data available for the damping of the structure-borne sound nor the spectrum and the amplitude of that sound a measurement series was performed on the test track of the RWTH-Aachen.

For the initial measurement series two different accelerometers, one from Jülich research center and a Brüel & Kiaer 4507 piezoelectric accelerometer, have been used. For the measurements both accelerometers have been connected to preamplifiers. Therefore, these preamplifiers are part of the

measurement setup. In consequence the recorded data includes this pre amplification. To ensure the accuracy of the measurements these accelerometers have been calibrated at the institute for technical acoustics. Their sensitivity has been determined to 2270 mVs²/m (for the sensor from Jülich) and 316 mVs²/m (for the Brüel & Kjaer 4507), respectively. Both accelerometers have been glued to the test track, as shown in Fig. 3, to guarantee a good coupling to the track and low damping for the structure-borne noise. The left accelerometer on the photo is the sensor from Jülich research center, the right one is the B & K 4507. Both accelerometers are sensitive to deflection in the z-axis.

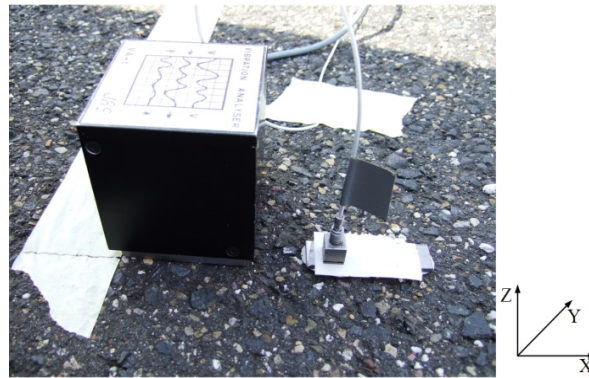


Fig. 3. Accelerometers used for the measurements [5].

The measurement setup, which was used during the initial measurement series, is illustrated in Fig. 4. The analog output voltages of the accelerometers have been recorded with a 24 Bit ADC at a sampling rate of 44.1 kHz. For the measurement series a car was driven past the accelerometers with a specified velocity and the distance, at which the left tires passed the accelerometer, was recorded manually. Table 1 shows some examples of the preformed measurement combinations of velocity and distance. The detection of the passing car was possible with both sensors, but due to its superior performance only the results from the accelerometer from Jülich Research Center will be discussed in the following section.

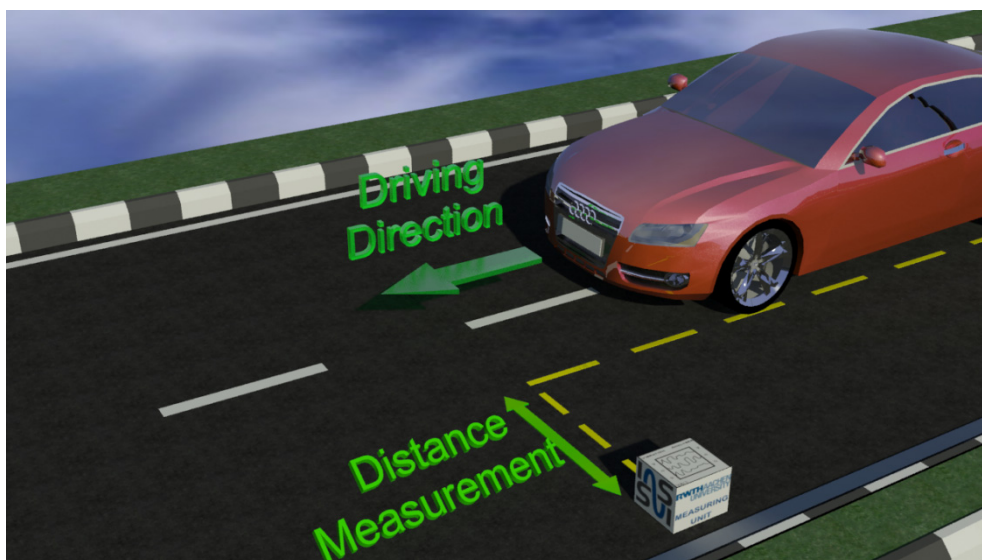


Fig. 4. Measurement Setup at the test track.

Table 1. Example of preformed measurements.

Velocity	Distance
25 km/h	25 cm
30 km/h	50 cm
40 km/h	30 cm
50 km/h	25 cm
50 km/h	30 cm
80 km/h	30 cm
100 km/h	75 cm

Fig. 5a shows the accelerometer's output for a passing car with 50 km/h at a distance of 30 cm. The peaks in the acceleration show the points when the car's axes passes the sensor and are clearly distinguishable from the noise floor despite of the overall low acceleration of roughly 4 mg. The detection of passing vehicles using their structure-borne noise signals poses several challenges for the read-out circuit. The signal to noise ratio of the acceleration signal is quite low especially for low velocity and large distance of the passing vehicle. Furthermore the output signal of the sensor can only be sampled for 1 ms at maximum due to the limited power resources of the sensor nodes. Fig. 5b shows an enlargement of the peak acceleration from Fig. 5 and 1 ms in scale to show that the passing vehicles have to be detected with only a part of a flank of the oscillation signal.

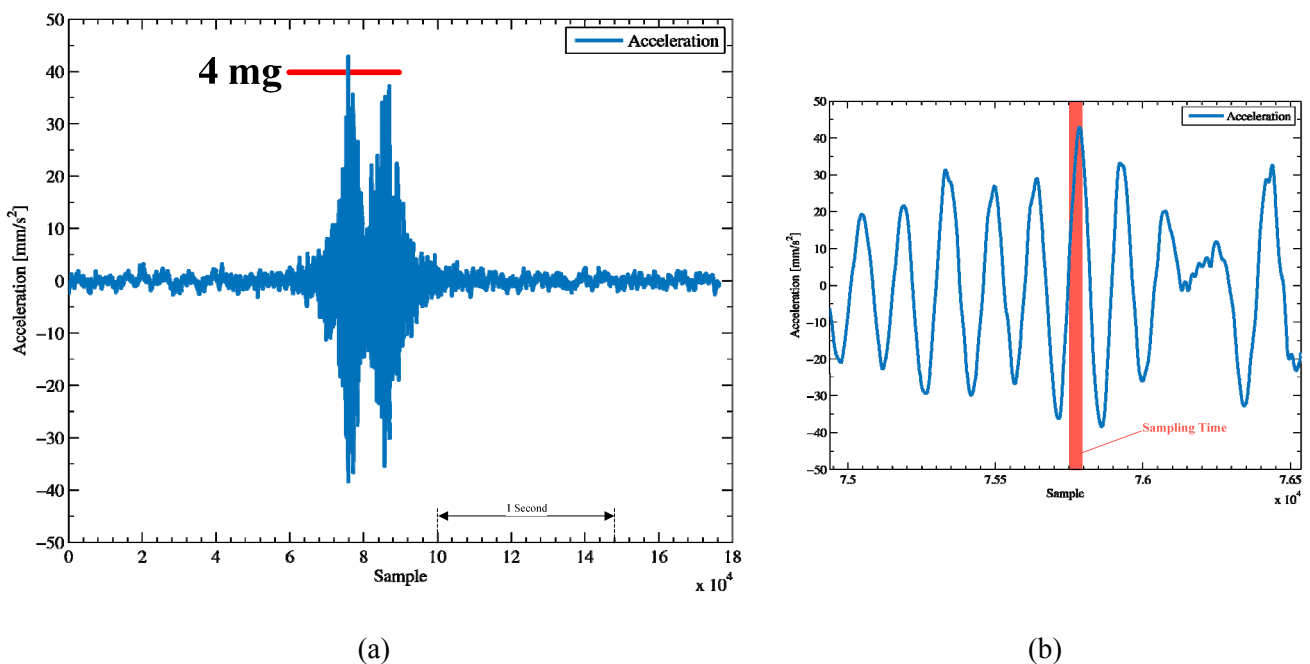


Fig. 5. Car passing the accelerometer with 50 km/h at 30 cm distance (a) and zoom at the peak of the acceleration signal (b) [5].

In order to reduce the amount of transmitted data, preprocessing is needed inside the sensor node. This preprocessing has to be able to detect all kind of passing vehicles at different speeds and distances from the sensor within 1 ms sampling time. To proof the feasibility of this task a straight forward filter, which is depicted in Fig. 6, has been developed. Fig. 7 shows the results of the filter at different stages. After the removal of the noise by a dead zone element and the differentiation of the signal the peaks in

the acceleration signal are distinguished from the noise. The last stages of the filter increase its accuracy. The filter was tested for a periodic operation of 10 ms and a sampling time of 1 ms using all recorded measurement data. It was able to detect both axes in every data set starting from random points in time.

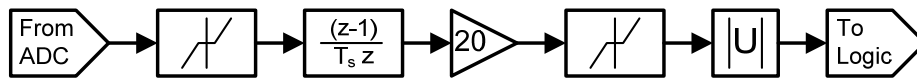


Fig. 6. Digital filter for vehicle detection [5].

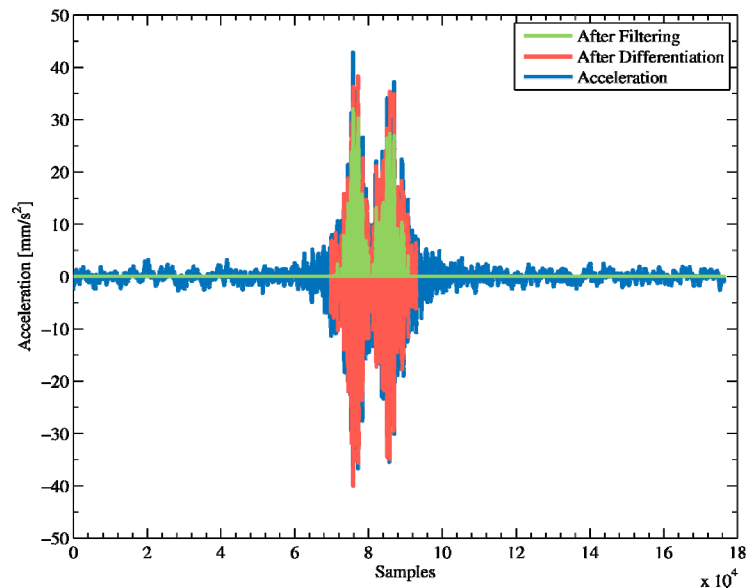


Fig. 7. Results of the different filter stages for a passing car with 50 km/h at 30 cm distance [5].

4. Sensor Node

Before an architectural study on the sensor node including the accelerometer and its readout circuit can be conducted, a decision on the power source for the sensor node has to be made. A power distribution between different sensor nodes and the beacons at the side of the road requires a lot of wires and is very error prone. Furthermore it is the most cost-intensive solution. For this reasons only local power sources, which do not need any power distribution between different sensor nodes, are taken into account. For finding the optimal energy source under these circumstances a short survey on all available and eligible energy sources was performed.

Obviously, the structure-born noise of passing vehicles can be used as an energy source for the sensor node. Since the structure-borne noise is a broadband acceleration, no resonant vibration energy harvesting devices can be used. Corresponding to the model for vibration energy harvesting from [6] the amount of power from low accelerations is very limited. Assuming the average acceleration is 10 mm/s², less than 10 μW could be harvested out of a volume of 100 cm³. Taking into account that this energy source shows large fluctuations since the structure-born noise depends on the passing vehicle, a large energy storage would be needed to ensure a safe power supply. Due to these drawbacks no further research has been performed on vibration energy harvesting as primary energy source for the sensor nodes.

Thermoelectric generators represent another possible energy source for the sensor node. These devices generate power out of a temperature difference utilizing the Seebeck effect. In a volume of 0.08 cm^3 for a temperature gradient of 5 K, $30 \mu\text{W}$ could be harvested [7]. It is very unlikely that temperature gradient of more than fractions of a Kelvin exist inside the car-pad layer over a useful amount of time since it is a uniform material of less than 1 cm thickness which will heat up homogeneously to the ambient temperature. Any temperature difference between the car-pad and the surrounding air is difficult to utilize, because large surface with direct contact to the passing vehicles would be needed. Furthermore it has to be taken into account that the harvestable power from thermoelectric generators shows a linear dependence to the temperature gradient leading to a volume of more than 100 cm^3 , which is needed for 1 mW output power at 0.1 K temperature gradient [6]. For this reason thermoelectric generators have not been selected as primary energy source for the sensor nodes.

Another possible energy source could be found in primary non rechargeable batteries which are nowadays available with the required milliampere hours and a lifetime of 10 years [8]. The environmental conditions for the sensor nodes in the car-pad are very harsh. Especially the high temperatures during direct solar irradiation in the summer month may cause a strong degradation of e.g. lithium ion batteries. For an increase of the average temperature from $20 \text{ }^\circ\text{C}$ to $40 \text{ }^\circ\text{C}$ a reduction of 70 % in the average lifetime was reported in [9]. Other primary battery technologies show similar reductions in lifetime, if they are exposed to higher temperatures. Furthermore an exchange of the batteries is not feasible due to too high expenses and the recycling of the batteries at their end of life would cause additional costs. The battery lifetime would limit the lifetime of the whole system and become a very critical issue. Due to these reasons primary batteries have not been selected as energy source for the sensor nodes.

Photovoltaic cells offer in combination with a sufficient large energy storage, a reliable and independent power supply. The solar irradiation can be up to 100 mW/cm^2 and its average value is 11 mW/cm^2 in Germany. Photovoltaic cells with an efficiency of 10 % and an active area of 1 cm^2 can provide an average power of 1.1 mW [10]. Since small solar cells can be integrated into the top layer of the road and offer sufficient power they have been selected as primary energy source. The exact dimensioning of the solar cell will be covered in section 5.1.

The structure of the sensor node to be integrated in the top layer of the road is shown in Fig. 8. The power supply of the sensor node consists of series connected solar cells, power regulators, an energy storage and a power management unit. A MEMS (Microelectromechanical System) accelerometer is the primary sensor of the node to detect the structure-born sound of passing vehicles. Further sensors for temperature and humidity can also be attached to the ASIC. Only the solar cells, the supercapacitor, the antenna and the accelerometer sensing element are external components. All other functions are fully integrated into the ASIC. Employing this method in consequence reduces the sensor node's dimensions, its power consumption and its price.

The cross section of a sensor node, which is integrated into the top layer of the road is shown in Fig. 9. A thin, but stiff glass panel protects the solar cell from mechanical stress. The solar cells are stacked onto the super capacitor, which is used for energy storage. The super capacitor and the ASIC are mounted and connected with a PCB. For reducing the dimensions of the sensor node the ASIC and MEMS sensor share a package. The whole sensor node will be protected by an epoxy encapsulation.

For an exact dimensioning of the sensor node and especially its power supply detailed specifications have to be derived. The requirements for the intelligent road infrastructure are the following: Vehicles with velocities from 5 km/h up to 180 km/h have to be detected and localized. For vehicles within a traffic jam (speed of less than 5 km/h) only the presence has to be detected. To minimize the consumed energy for the sensor node operation, a periodic operation mode has been designed. Based on the

measurements it is expected that each sensor node can detect vehicles within a radius of 50 cm. Therefore, the sensor node mesh has been designed to a distance of 1 m between each node. Taking into account this distance and the maximal detectable speed of passing vehicles the minimal duty cycle for periodic operation is 0.09. This leads to a required activation of the accelerometer every 20 ms for a detection range for the sensor of 50 cm.

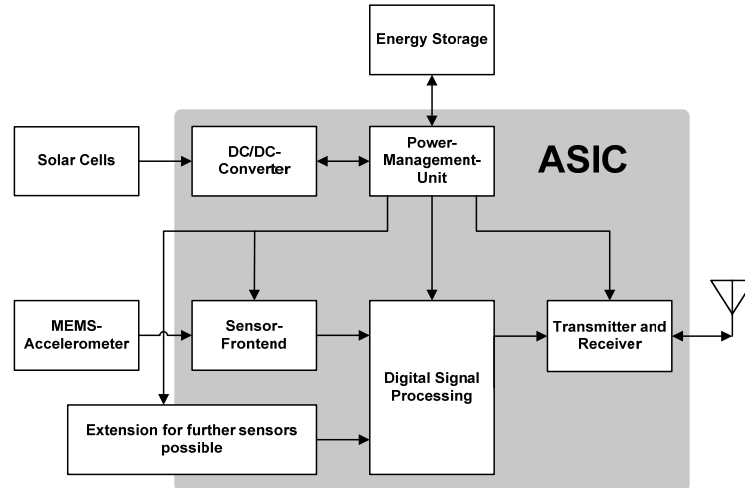


Fig. 8. Structure of the sensor node.

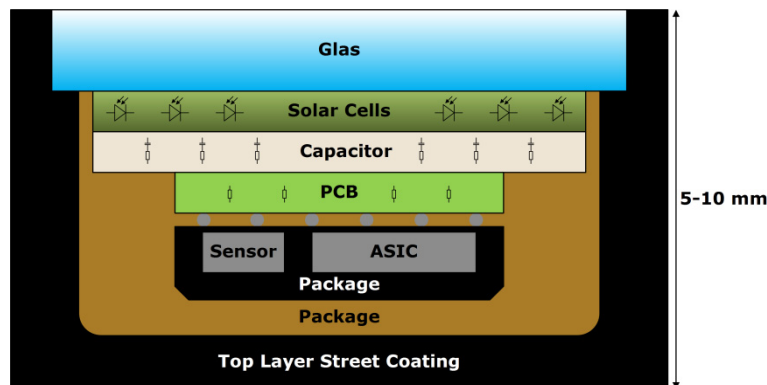


Fig. 9. Cross section of a sensor node integrated into the car-pad.

The specifications for the periodic operation mode provide the basis for an estimation of the required energy for one activation. This coarse approximation neglects the losses in the power management unit, the DC/DC converter and the leakage currents of the energy storage. Table 2 shows the approximation of the necessary power for the different building blocks and the reference, on which basis this data has been calculated. All building blocks are feed by a single 3.3 V supply. The sensing element is purely passive and therefore does not consume any energy. The sensor frontend includes the driver for the sensing element and is active for more than 1 ms and needs about 1.8 μJ per activation. The analog to digital converter (ADC) is active as long as the sensor frontend is active and is very energy efficient due to low sampling frequency and reasonable resolution. The energy required for the digital signal processing is estimated to 0.3 μJ , since this can be done in parallel in only a few hundred clock cycles. Transmitting the information to the beacon at the side of the highway consumes about 2.4 μJ . In total about 5 μJ are required for one activation of the sensor node. Fig. 10 illustrates the approximated required current and energy for the sensor node over time. The power supply was designed to provide 1 mA out of 3.3 V supply for 2 ms for assuring a safety margin for the

implementation. Taking into account that an amount of $6.6 \mu\text{J}$ is required every 20 ms an average power of $330 \mu\text{W}$ is enough to supply the sensor node.

Table 2. Estimation of the required energy for one activation of the sensor node.

Functional block	Power	Required energy	Reference
Sensing element	- (passive)	-	
Sensor frontend	$1320 \mu\text{W}$	$1.8 \mu\text{J}$	[11]
Analog to digital converter	$165 \mu\text{W}$	$0.2 \mu\text{J}$	[12]
Digital signal processing	$3300 \mu\text{W}$	$0.3 \mu\text{J}$	
Transmitter	$7600 \mu\text{W}$	$2.4 \mu\text{J}$	[13]
Total		$4.7 \mu\text{J}$	
Total with security margin		$6.6 \mu\text{J}$	

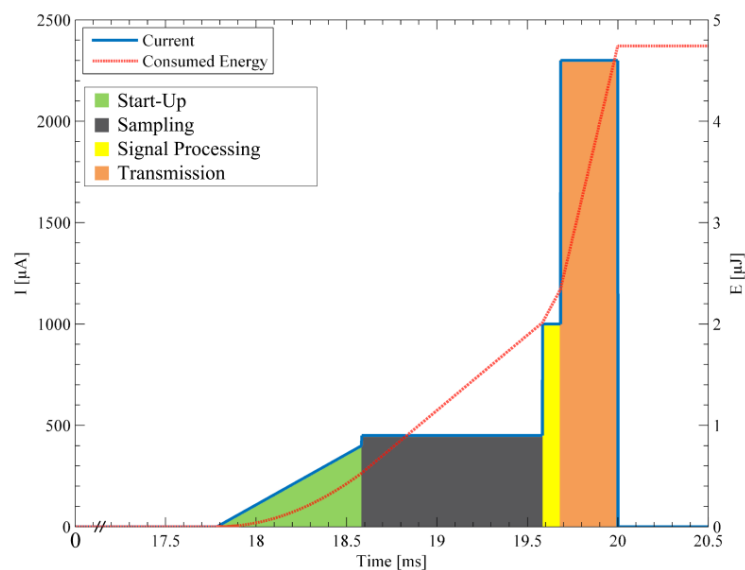


Fig. 10. Approximated required current and energy of the sensor node over time.

5. Power Supply Sensor Node

The power supply for the sensor node inside the top layer of the road is a critical issue. A lifetime of 10 years is targeted for the top layer of the road. Therefore, it is necessary that the sensor node can operate for an even longer period of time. As shown in the previous section, solar cells are the optimal energy source for the sensor nodes inside the car-pad and offer the highest energy density for this application. Furthermore they are well studied and available for low cost. Their only drawback is the need for a transparent package with low reflection to maximize the irradiated power for the solar cell. To keep the sensor node operating during night or times, when the solar cell is covered with e. g. snow, an energy storage is required. In addition a power management unit is needed to control the electronics to maximize the harvested energy and the operation time of the sensor node.

5.1. Solar Cell

Today different types of solar cells based on diverse materials like monocrystalline silicon or organic polymers are available. In comparison to other semiconductor types, silicon thin film solar cells offer

medium efficiencies of more than 10 %, low price and long term stability [10]. Furthermore the efficiency of amorphous silicon is quite constant, even for weak irradiated powers [14]. To consider the life time degradation and shadowing effects an efficiency of only 7.8 % is assumed for the power supply dimensioning calculation.

5.2. Energy Storage

The output power of the photovoltaic cells depends on the irradiated power, which varies strongly in this application. Therefore, an energy storage is required to supply the sensor node with enough energy, if the solar cell cannot power it on its own. For this application, the specific energy and the number of charge-discharge cycles are the most important parameters for the energy storage. The specific power is not important, because the sensor node uses less than 7 mW peaked. Li-ion rechargeable batteries and supercapacitors are the most promising energy storage technologies for these demands [15]. Due to the harsh temperature range from -40 to 80 °C in this application batteries are not suitable, because their capacity would drastically decrease within the first years of operation [9]. That is why supercapacitors have been chosen as energy storage technology. They do not limit the lifetime of the sensor node nor lose much capacity due to the temperature range.

5.3. Power Management System

Besides the energy source and storage DC/DC-converters are required to improve the available power for the sensor node. A direct connection of the solar cell to the ASIC with the supercapacitor in parallel would not work, because the supply voltage would change between 0 V and the open circuit voltage of the solar cells. Therefore, the power supply concept depicted in Fig. 11 was developed. Several solar cells, which are connected in series to increase the output voltage, power the sensor node. A multiplexer can connect the supercapacitor or the solar cells to a charge pump. As a substitute of directly connecting the solar cells to the load, a charge pump keeps the cells in their maximum power point. This can increase the harvested energy by more than 25 % despite of the losses in the charge pump [8]. The output energy from the charge pump can be used to charge the supercapacitor or directly power the low drop out regulator (LDO). Using the Multiplexer (MUX) and Demultiplexer (DEMUX) lowers the efficiency for the direct connection due to resistive losses. Since both MUX and DEMUX switch infrequent, the transistors can be quite large minimizing the resistive losses. These multiplexers are used to enable four different operation modes. The first one is used to charge the supercapacitor with the energy out of the solar cells. In this mode the charge pump performs the maximum power point tracking and can increase the output voltage of the solar cells to utilize the full voltage range (up to 5 V) for the supercapacitor and maximize the stored charge. The ASIC is powered in the second operation mode from the supercapacitor. A LDO stabilizes the power supply voltage. Since the losses in the LDO are proportional to the voltage drop across it, the charge pump minimizes it, by keeping the input voltage of the LDO only slightly above the LDO's dropout voltage. The ASIC can also be direct powered via the charge pump and the LDO, if the output power of the solar cells is sufficient. Furthermore a mixed supply from the solar cells and the supercapacitor for the ASIC is possible, too.

The power supply of the sensor node has been designed for an operation in Germany, but by adapting the solar cell area and supercapacitor size it can be used all over the world. The ASIC has to be active every 20 ms for 2 ms to be able to detect passing vehicles with a speed up to 180 km/h. During its active phase the ASIC needs less than 6.6 μ J. Therefore, it consumes maximal about 250 mWh per month.

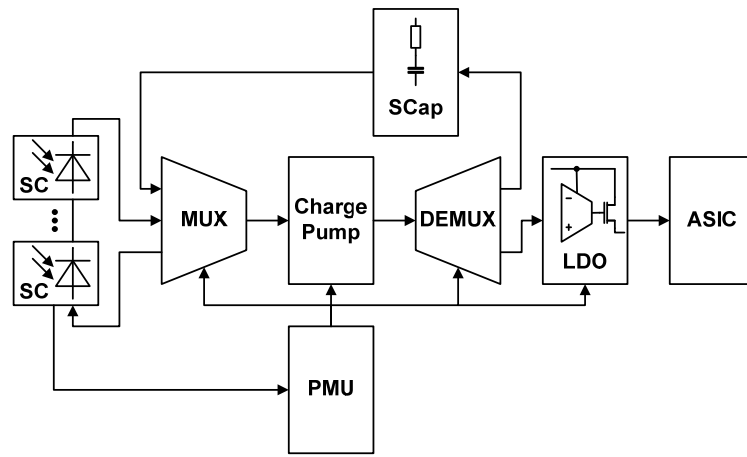


Fig. 11. Power Supply Sensor Node [5].

For checking the feasibility of the sensor node power supply an estimation of the required solar cell area was performed. Fig. 12 shows the average sunshine duration for a meteorological winter from 1951 to 2008 in Germany. The meteorological winter in Germany includes the months from December till February. This period of the year has been selected, because these are the months with the least sunshine duration. Sunshine duration is defined as a time interval, in which the irradiated power of the sun is greater than 120 W/m^2 [16]. From Fig. 11 can be derived that the average sunshine duration per month in the metrological winter is 50 hours. The minimal value has been measured in 1970 with an average of 34.7 hours per month. It has been assumed that the solar cells are exposed to at least 50 hours with an irradiated power of at least 180 W/m^2 every month in order to ensure a realistic sizing. The increased value of 180 W/m^2 compared to the sunshine duration definition of at least 120 W/m^2 has been chosen since an irradiated power of more than 180 W/m^2 can be expected even for cloudy day during metrological winter.

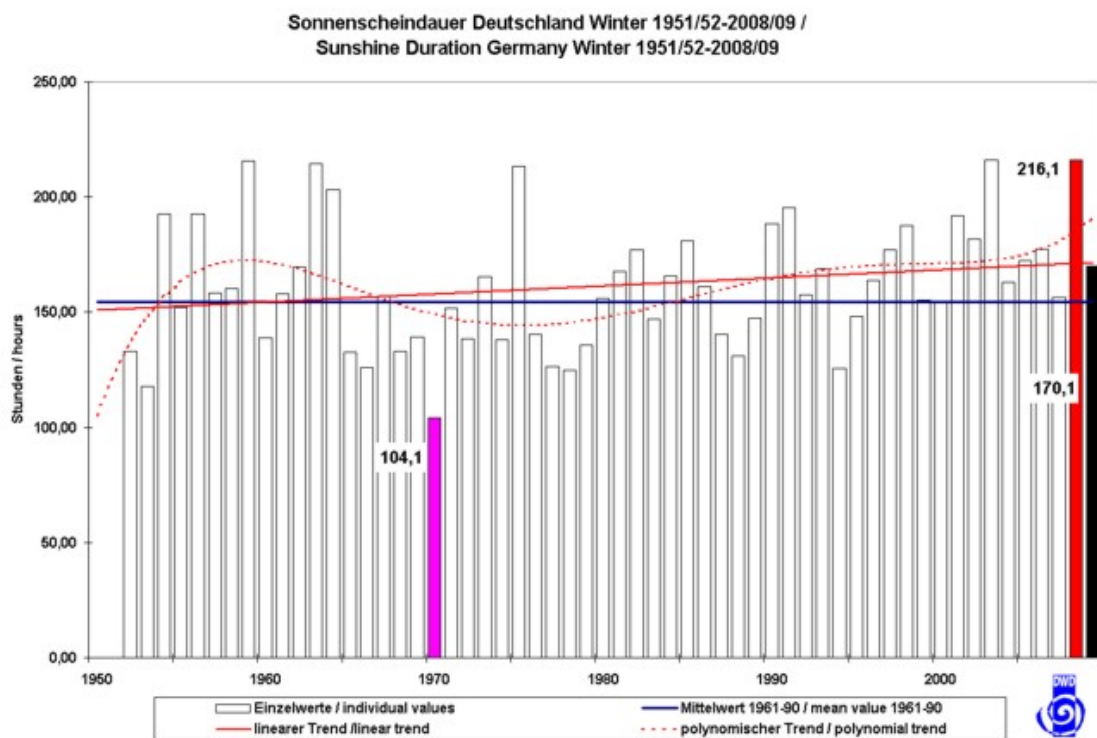


Fig. 12. Average sunshine duration during the meteorological winter in Germany [17].

For the approximation of the solar cell area, shadowing effects, such as dirt spots on the covering glass, have been taken into account by lowering the solar cell efficiency by 25 %. This assumption is reasonable, since pollution of the protection glass is only a minor problem due to the large amount of rain in Europe [18]. Furthermore the passing vehicles, which drive over the sensor node, clean its surface. The actual shadowing, e.g. due to passing cars, is hard to estimate, but the reduction of 25 % and the conservative approximation of the irradiated power offer an adequate security margin to compensate this losses.

The influence of the operating temperature of the solar cells on its efficiency has not been taken into account for the estimation of the required solar cell area. The solar cells and their surrounding car-pad layer mainly heat up due to direct solar irradiation. This means, if the efficiency of the solar cells drops due to an increase in the ambient temperature, the irradiated solar power will be well above 180 W/m². Due to this fact the overall energy output of the solar cells will be much higher, although their efficiency has dropped. For this reason the estimation has been conducted using a low irradiation operation point of the solar cells (180 W/m²) [18]. For a required power of 250 mWh per month an area of 6 cm² is sufficient to power the sensor node for the given assumptions. The solar cell area can be utilized more efficient, if 6 solar cells of 1 cm² are used instead of one large solar cell of 6 cm². By connecting these 6 solar cells in series their output voltage can be increased and the efficiency of the charge pump can be maximized.

For ensuring that the above stated estimation of the solar cell area is valid, a second estimation has been performed based on the method of [19]. An average irradiated power of 0.69 kWh/m² per day can be calculated using equation (1) for an availability of 95 % for the area around Aachen in Germany [19].

$$G_{dim}(\bar{a}) = GA \cdot \left(1 - \frac{\bar{a} - 1 + \left(\frac{\sigma}{GA \cdot \sqrt{2\pi}} \right)}{\frac{1}{2} - \frac{\sigma}{GA \cdot \sqrt{2\pi}}} \right). \quad (1)$$

For this calculation the data out of [19] for the region around Aachen in Germany with an average irradiated solar power GA of 2.76 kWh/m² per day and a standard deviation σ of 1.68 kWh/m² per day has been employed. G_{dim} is the irradiated power per day which is exceeded for the given percentage of the year (\bar{a}). The area of the solar cells can be reduced to 3 cm² for the calculated average irradiated power of 0.69 kWh/m² per day for an efficiency of 7.88 % of the solar cells. Therefore, the above estimated 6 cm² is a real conservative calculation, which will guaranty the full functionality of the intelligent road infrastructure under all weather conditions.

Based on the estimation of the energy output of the solar cells the other parts of the power supply for the sensor node could be dimensioned. The efficiency of the charge pump is assumed to be 90 % with a quiescent current of 2 μ A. Taking the production variations and degradation over the lifetime into account the supercapacitor size has been set to 106 mF, which is more than 40 % larger than needed. The size of the energy storage enables the sensor node to operate in total darkness for 31 days, which should ensure operation even during winter with a lot of snow. A more detailed design based on exact data will lead to a drastic size reduction for the solar cell and the energy storage, which will lower the price per sensor node.

6. Transmitter

The transmission of the sensor data from the sensor node to the base station has to be wireless, since a wired transmission would be too complex and expensive. For an approximation of the required energy for the data transmission the data packets and the attenuation have to be estimated. One data packet needs to consist of an ID, the sensor data and a checksum. It can be dimensioned to be less than 256 bit. The ID for every sensor node is required to enable the beacon to distinguish between different sensor nodes and derive the local traffic situation. The frequency band for the data transmission should be selected below 1 GHz due to the better propagation properties. Therefore, the frequency ranges 869.40-869.65 MHz or 869.70-870.00 MHz have been selected for the data transmission.

The estimation of the attenuation of the link between the different sensor nodes and the base station located in the beacons at the side of the highway is based on the configuration shown in Fig. 13. It has been assumed that the distance between 2 beacons is 50 m and that a beacon has to cover at maximum 3 lanes. Based on the dimension given above and in Fig. 13 the maximum distance between a sensor node and the beacon is 29.2 m. The angle α is small which leads to a propagation path of 14 cm through the top layer of the highway and an attenuation of 62 dB for the direct path. Considering the optimal indirect propagation path only 5 mm of the top layer have to be traversed leading to an attenuation of 61 dB. The difference between these propagation paths is shown in Fig. 14. Since the composition of the top layer is still under intensive investigation for both calculations the absorption coefficient inside the top layer of the road has been assumed to be equal to 1.67, the absorption coefficient of concrete [20].

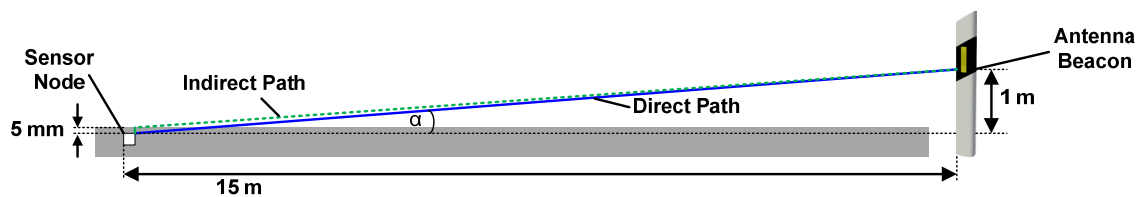


Fig. 13. Propagation path for a transmission of a sensor node to the base station [5].

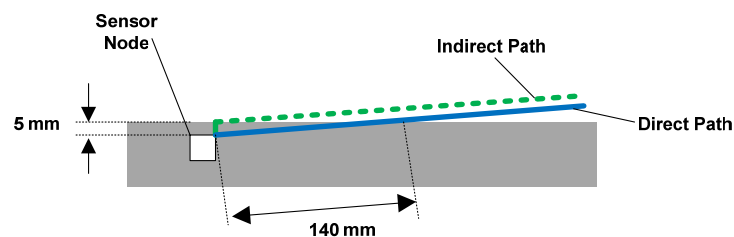


Fig. 14. Zoom to the difference between the direct and indirect propagation path [5].

Both antennas have been assumed to radiate omnidirectional for ensuring a cost efficient antenna design. Using antennas with a directional radio pattern in the beacon may further reduce the required output power of the transmitter but has not been taken into account in this paper. An output power of 0.5 mW (-3 dBm) for the sensor node leads to a power of 392 pW (-64 dBm) at the antenna of the base station. This input power level can be energy efficient and cost effective received [13]. Furthermore it has to be taken into account that the base station will have more power available than the sensor nodes. For estimating the required power for a transmission of one data packet from a sensor node to a beacon several published transmitters have been compared in Table 3. To take the special requirements for the

car-pad into account the output power of all transmitters have been linearly scaled to -3 dBm and the power for a whole burst (energy per data packet) has been compared. If no start up time for the transmitter has been published in the reference mentioned below, it has been assumed to be 1 ms. The most energy efficient transmitter for the data transmission from a sensor node to a base station is to the knowledge of the author [13], which requires only 2.4 μJ per transmission of one data package. This is equal to a power of 7.6 mW for 316 μs .

Table 3. Comparison of different transmitters.

Center Frequency	Data rate	Energy per data packet	Reference
916.5 MHz	1 Mbit/s	2.4 μJ	[13]
900 MHz	100 kbit/s	9.3 μJ	[21]
868 MHz	100 kbit/s	5.3 μJ	[22]
433 MHz	100 kbit/s	8.9 μJ	[23]

7. MEMS Accelerometer

Detecting the structure-borne noise of passing vehicles on a highway imposes several challenging requirements for the sensing element, like mg resolution in combination with ultra low power consumption. To the knowledge of the authors the required resolution can be attained with the following type of sensing: piezo-resistive, capacitive, thermal, tunneling and optical. Especially sensing using tunneling current or optical measurements of acceleration is very exact and a resolution up to ng is feasible [24]. Due to the large volumes and high costs of these approaches these sensing techniques have not been selected for the integration into the car-pad. For this application an accelerometer which easy fits inside the top layer of the road and can be produced in large amounts of more than 1 million devices per year with constant quality for a reasonable price, is required. Thermal sensing is not taken further into account, since batch production is quite difficult for this type of accelerometer [24]. In comparison to piezo-resistive sensing, capacitive accelerometers are the better choice with regard to the special requirements of the sensor nodes inside the car-pad. Capacitive MEMS accelerometer show less temperature drifts and can be build within a smaller volume than piezo-resistive ones [24]. Furthermore they have been used for decades in the automotive industry and their long term stability of more than 10 years has been proven with several devices. Their shortcomings, such as great parasitic capacitances, can be compensated with integrated read out circuits like the one presented in section 8. Therefore, capacitive MEMS have been selected as sensing technique for this application.

It is very important to understand the special properties of capacitive MEMS accelerometers to read out the maximal achievable resolution with a certain device. Fig. 15 shows an electron microscopy picture of a single axis capacitive accelerometer. Its electrical performance can be approximated with the circuit shown in Fig. 16. An acceleration leads to a relative deflection of the seismic mass and the frame, which can be detected by a change in differential capacitance between the finger of these structures (C_1 and C_2). This change in capacitance can be readout e.g. by driving the ports 1 and 2 while reading out the change of the charge on port M. Due to the small dimensions of the accelerometer the influence of the parasitic couple capacitance and the parasitic capacitance to the substrate cannot be neglected. The finite conductance of the polysilicon connections causes parasitic resistances, which are about a few kilo ohms and build a lowpass with the different capacitances. For maximizing the achievable resolution not only reducing these parasitics, but also optimizing the mechanical properties is important. Therefore, the stiffness of the springs, which connect the seismic mass to the frame, should be matched to the application. Furthermore not only the electrical but also the mechanical noise has to be taken into account. Due to their small size capacitive MEMS

accelerometers have a light weighted seismic mass, which causes a high mechanical noise floor limiting the achievable resolution. The initial measurements on the test track have shown that the required resolution for the sensor nodes is at least 1 mg, which can be achieved with MEMS accelerometers [25]. The challenge for this application is to maintain the required resolution with as little power consumption as possible and for a competitive price. Therefore, the MEMS accelerometer has to be optimized for the structure-borne sound detection to lower the requirements for the readout circuits and its power consumption.

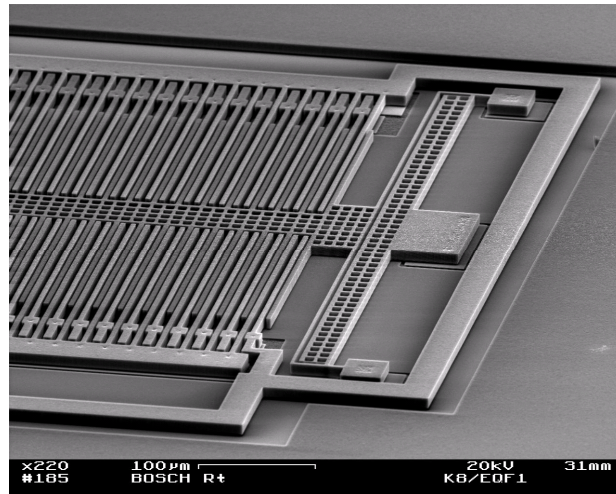


Fig. 15. Picture of a single axis capacitive MEMS accelerometer provided by Robert Bosch GmbH.

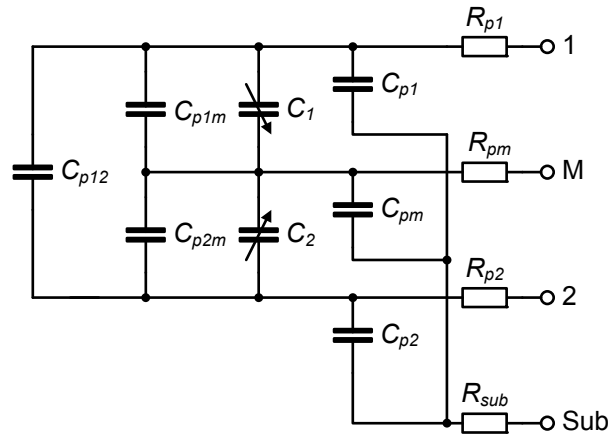


Fig. 16. Electrical model of a capacitive MEMS accelerometer [5].

8. Sensor Frontend

One main challenge of the sensor node design for the intelligent road infrastructure is the power efficient readout of the capacitive MEMS accelerometer. For small parasitic capacitances at the readout node of the sensing element continuous time voltage sensing (CTV) is superior to other readout techniques, such as switched capacitor [26]. Furthermore it shows a better performance for low power readout circuits, because the resolution is not limited due to noise folding. Different time continuous readout circuits have been compared for finding the optimal readout circuit for the special requirements of the integration inside the car-pad [5, 27]. The readout circuit, which was expected to perform best, has been selected and designed to meet the requirements for this application [5, 28].

The accelerometer readout circuit is based on [25, 29] and uses dual-chopper stabilization for noise and offset reduction as well as power saving. As depicted in Fig. 17, the frontend uses energy efficient square wave stimulation with the frequency PHH convoluted with PHL on port 1 and 2 of the sensing element. The acceleration dependent charge variations are evaluated on the middle port (M) of the sensing element. The first operational amplifier converts the charge into a voltage and adds flicker noise and offset to the signal. Its gain can be selected with the *gain0* and *gain1* switches. A passive mixer is used to mix the signal down from $\text{PHH} \pm \text{PHL}$ to PHL. Since the flicker noise and offset is around DC, it is mixed up to PHH and apart from the signal. The second operational amplifier further boosts the signal and is more energy efficient, since it operates at lower frequencies. After the second mixer the signal is mixed to DC and the noise is at PHL and $\text{PHH} \pm \text{PHL}$, respectively. Therefore, the noise can be reduced with a lowpass filter. The signal is digitized with an analog to digital converter.

To increase the resolution different calibration cycles are intended in the readout circuit. The sensor offset, which can drive the sensor frontend into saturation, is coarse reduced with a capacitor array at the middle port of the sensing element. A fine reduction is achieved with a DAC in the input stage of the second operational amplifier (not depicted in Fig. 17). Furthermore the gain and offset for other building blocks are calibrated. To achieve the needed resolution of 1 mg a gain of more than 60 dB is required, which limits the input acceleration range to less than 1 g. The gains of both operational amplifiers are controlled by the logic to keep the frontend from saturating and therefore increase the acceleration input range.

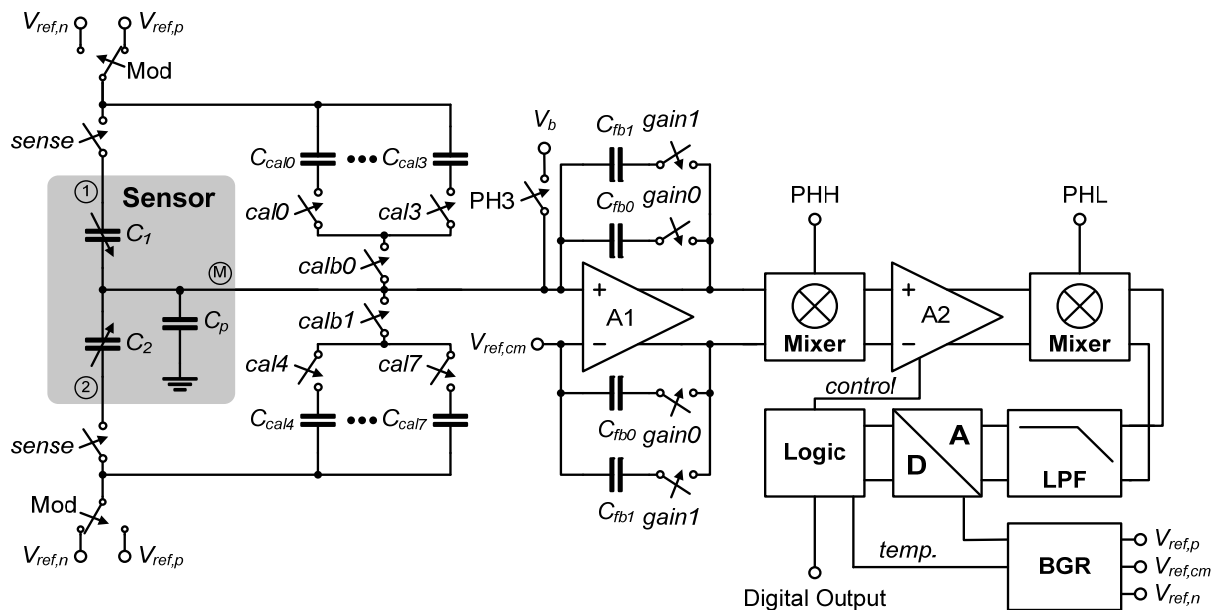


Fig. 17. Accelerometer time continuous readout circuit [5].

9. Conclusions & Outlook

This paper shows a promising concept of an intelligent road infrastructure. With this approach the traffic situation can be determined without having special equipped cars. Due to the absolute and accurate position information of each car, an exact traffic situation can be derived. Traditional navigation systems extended with a receiver can be used as vehicle on-board units. The system can not only be used for optimal routing but also to enhance security by giving drivers assistance and warnings.

It has been shown in a measurement series that structure-born sound can be used to detect vehicles and

their speed. The proposed sensor net can easily be integrated with low costs into an industrial fabricated "rollable" road, called car-pad. We have presented the sensor node on block level including detailed specifications. These specifications have been verified by reported circuitries listed in literature or by own transistor level simulations.

Further research on the MEMS accelerometer is ongoing [30]. In addition to this, a capacitive MEMS accelerometer readout circuit will be developed on circuit level and a test chip for the whole frontend is planned for the next years [31, 32].

Acknowledgements


The work on the system concept has been supported by the Institute of Road and Traffic Engineering (IASC) of the RWTH-Aachen.

References

- [1]. Houben, L. J. M., van der Kooij, J., Naus, R. W. M. & Bhairo, P. D., APT testing of modular pavement structure 'Rollpave' and comparison with conventional asphalt motorway structures, *Accelerated Pavement Testing*, 2004, pp. 1-24.
- [2]. Groenendijk, J. & Westera, G., Proefvak rollpave A35. Final report, *Innovatieprogramma geluid voor weg- & spoorverkeer (iPG)*.
- [3]. Deutschle, S., Kessler, G., Lank, C., et al. M., Einsatz elektronisch gekoppelter LKW-Konvois auf Autobahnen, *ATZ - Automobiltechnische Zeitschrift*, 2010.
- [4]. Wunderlich, R., Strache, S., Busen, C., et al., Intelligent road infrastructure - a concept study, in *Proceedings of the SENSORCOMM*, 2011, pp. 1-5.
- [5]. Strache, S., System approach for an embedded accelerometer read-out circuit, Diploma Thesis, *RWTH-Aachen University IAS*, 2009.
- [6]. Roundy, S., Steingart, D., Frechette, L., Wright, P. & Rabaey, J., Power sources for wireless sensor networks, *Springer Berlin/Heidelberg*, Vol. 2920/2004, 2004, pp. 1-17.
- [7]. Paradiso, J. & Starner, T., Energy scavenging for mobile and wireless electronics, *Pervasive Computing, IEEE*, Vol. 4, 1, 2005, pp. 18-27.
- [8]. Simjee, F. & Chou, P., Efficient charging of supercapacitors for extended lifetime of wireless sensor nodes, *IEEE Transactions on Power Electronics*, Vol. 23, 3, 2008, pp. 1526-1536.
- [9]. Perrin, M., Malbranche, P., Lemaire-Potteau, E., et al., Temperature behaviour: comparison for nine storage technologies: results from the INVESTIRE network, *Journal of Power Sources*, Vol. 154, 2, 2006, pp. 545-549.
- [10]. Green, M. A., Emery, K., Hishikawa, Y. & Warta, W., Solar cell efficiency tables (version 36), *Prog. Photovolt: Res. Appl.*, Vol. 18, 5, 2010, pp. 346-352.
- [11]. BMA 150 Digital, Triaxial, Acceleration Sensor, 2008.
- [12]. Kim, H., Min, Y., Kim, Y. & Kim, S., A low power consumption 10-bit rail-to-rail SAR ADC using a C-2C capacitor array, in *Proceedings of the IEEE International Conference on Electron Devices and Solid-State Circuits (EDSSC' 08)*, 2008, pp. 1-4.
- [13]. Daly, D. & Chandrakasan, A., An energy-efficient OOK transceiver for wireless sensor networks, *EEE Journal of Solid-State Circuits*, Vol. 42, 5, 2007, pp. 1003-1011.
- [14]. Reich, N., van Sark, W., Alsema, E., et al., Weak light performance and spectral response of different solar cell types, in *Proceedings of the 20th European Photovoltaic Solar Energy Conference*, 2005.
- [15]. Hall, P. J. & Bain, E. J., Energy-storage technologies and electricity generation, *Energy Policy*, Vol. 36, 12, 2008, pp. 4352 – 4355.
- [17]. Deutscher Wetter Dienst, Sonnenscheindauer Deutschland Winter 1951/52-2008/09, 2009.
- [16]. Guide to Meteorological Instruments and Methods of Observation, 7 edition, *World Metrological Organization*, 2008.
- [18]. Wagner, Andreas, Photovoltaik Engineering - Die Methode der Effektiven Solarzellen-Kennlinie, *Springer*, Berlin, 1999.

- [19].Wagner, Andreas, Photovoltaik Engineering: Handbuch für Planung, Entwicklung und Anwendung (VDI), Springer, Berlin, Vol. 2, 2008, pp. 337.
- [20].Maierhofer, C., Leipold, S. & Wöstmann, J., Sturkturuntersuchungen in Beton mit dem Impulsradar, DGZfP-Berichtsband 66, Vol. 66, 1999, pp. 47-57.
- [21].Molnar, A., Lu, B., Lanzisera, S., et al., An ultra-low power 900 MHz RF transceiver for wireless sensor networks, in *Proceedings of the IEEE Custom Integrated Circuits Conference*, 2004, pp. 401-404.
- [22].Enz, C., El-Hoiydi, A., Decotignie, J.-D. & Peiris, V., WiseNET: an ultralow-power wireless sensor network solution, *Computer*, Vol. 37, 8, 2004, pp. 62-70.
- [23].Boom, N., Rens, W. & Crols, J., A 5.0 mW 0 dBm FSK transmitter for 315/433 MHz ISM applications in 0.25 μm CMOS, in *Proceeding of the 30th European Solid-State Circuits Conference (ESSCIRC' 04)*, 2004, pp. 199-202.
- [24].Krishnan, G., Kshirsagarand, C. U., Ananthasuresh, G. K. & Bhat, N., Micromachined high-resolution accelerometers, *Journal of the Indian Institute of Science*, Vol. 87, 30, 2007, pp. 333-361.
- [25].Fang, D., Qu, H. & Xie, H., A 1 mW dual-chopper amplifier for a 50- $\mu\text{g}/\text{Hz}$ monolithic CMOS-MEMS capacitive accelerometer, *Digest of Technical Papers of the Symposium on VLSI Circuits*, 2006, pp. 59-60.
- [26].Yazdi, N., Kulah, H. & Najafi, K., Precision readout circuits for capacitive microaccelerometers, in *Proceedings of the IEEE Sensors Conference*, Vol. 1, 2004, pp. 28-31.
- [27].Strache, S., Wunderlich, R., Droste, D. & Heinen, S., Nichtlinearitäten in Ausleseschaltungen für kapazitive Nieder-g-Beschleunigungssensoren, *Sensoren und Messsysteme 2010 Vorträge der 15. ITG/GMA-Fachtagung vom 18. bis 19. Mai 2010 in Nürnberg*, VDE Verlag, 2010, pp. 55-62.
- [28].Strache, S., Wunderlich, R., Droste, D. & Heinen, S., MATLAB/Simulink model of a MEMS accelerometer read-out circuit, in *Proceedings of the EUROSENSORS XXIV Conference*, Linz, Austria, Elsevier BV, September 5-8, 2010, pp. 1-4.
- [29].Wu, J., Fedder, G. & Carley, L., A low-noise low-offset capacitive sensing amplifier for a 50- $\mu\text{g}/\text{Hz}$ monolithic CMOS MEMS accelerometer, *IEEE Journal of Solid-State Circuits*, Vol. 39, 5, 2004, pp. 722-730.
- [30].Rivas, J., Design of an Integrated Acceleration Sensor, Master thesis RWTH Aachen IAS/FH Aachen, 2011.
- [31].Schulte Bocholt, E. C., Development of an Operational Amplifier for Capacitive Accelerometer Readout Circuits, Bachelor thesis, RWTH-Aachen University IAS, 2011.
- [32].Bergert, J. M., Implementation of a Continuous Time, High Resolution Read-Out Circuit for Capacitive Accelerometers, Diploma thesis, RWTH-Aachen IAS, will be finished in December 2011.

2012 Copyright ©, International Frequency Sensor Association (IFSA). All rights reserved.
(<http://www.sensorsportal.com>)



Universal Frequency-to-Digital Converter (UFDC-1)

- 16 measuring modes: frequency, period, its difference and ratio, duty-cycle, duty-off factor, time interval, pulse width and space, phase shift, events counting, rotation speed
- 2 channels
- Programmable accuracy up to 0.001 %
- Wide frequency range: 0.05 Hz ... 7.5 MHz (120 MHz with prescaling)
- Non-redundant conversion time
- RS-232, SPI and I²C interfaces
- Operating temperature range -40 °C ... +85 °C

www.sensorsportal.com info@sensorsportal.com SWP, Inc., Canada

Guide for Contributors

Aims and Scope

Sensors & Transducers Journal (ISSN 1726-5479) provides an advanced forum for the science and technology of physical, chemical sensors and biosensors. It publishes state-of-the-art reviews, regular research and application specific papers, short notes, letters to Editor and sensors related books reviews as well as academic, practical and commercial information of interest to its readership. Because of it is a peer reviewed international journal, papers rapidly published in *Sensors & Transducers Journal* will receive a very high publicity. The journal is published monthly as twelve issues per year by International Frequency Sensor Association (IFSA). In addition, some special sponsored and conference issues published annually. *Sensors & Transducers Journal* is indexed and abstracted very quickly by Chemical Abstracts, IndexCopernicus Journals Master List, Open J-Gate, Google Scholar, etc. Since 2011 the journal is covered and indexed (including a Scopus, Embase, Engineering Village and Reaxys) in Elsevier products.

Topics Covered

Contributions are invited on all aspects of research, development and application of the science and technology of sensors, transducers and sensor instrumentations. Topics include, but are not restricted to:

- Physical, chemical and biosensors;
- Digital, frequency, period, duty-cycle, time interval, PWM, pulse number output sensors and transducers;
- Theory, principles, effects, design, standardization and modeling;
- Smart sensors and systems;
- Sensor instrumentation;
- Virtual instruments;
- Sensors interfaces, buses and networks;
- Signal processing;
- Frequency (period, duty-cycle)-to-digital converters, ADC;
- Technologies and materials;
- Nanosensors;
- Microsystems;
- Applications.

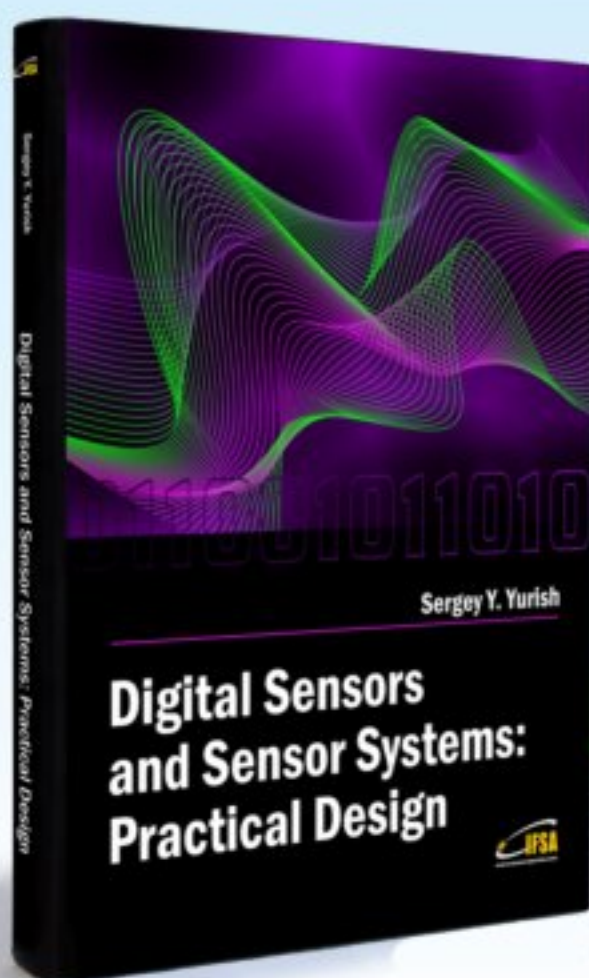
Submission of papers

Articles should be written in English. Authors are invited to submit by e-mail editor@sensorsportal.com 8-14 pages article (including abstract, illustrations (color or grayscale), photos and references) in both: MS Word (doc) and Acrobat (pdf) formats. Detailed preparation instructions, paper example and template of manuscript are available from the journal's webpage: <http://www.sensorsportal.com/HTML/DIGEST/Submission.htm> Authors must follow the instructions strictly when submitting their manuscripts.

Advertising Information

Advertising orders and enquires may be sent to sales@sensorsportal.com Please download also our media kit: http://www.sensorsportal.com/DOWNLOADS/Media_Kit_2012.pdf

Digital Sensors and Sensor Systems: Practical Design will greatly benefit undergraduate and at PhD students, engineers, scientists and researchers in both industry and academia. It is especially suited as a reference guide for practitioners, working for Original Equipment Manufacturers (OEM) electronics market (electronics/hardware), sensor industry, and using commercial-off-the-shelf components, as well as anyone facing new challenges in technologies, and those involved in the design and creation of new digital sensors and sensor systems, including smart and/or intelligent sensors for physical or chemical, electrical or non-electrical quantities.



"It is an outstanding and most completed practical guide about how to deal with frequency, period, duty-cycle, time interval, pulse width modulated, phase-shift and pulse number output sensors and transducers and quickly create various low-cost digital sensors and sensor systems ..." (from a review)

Order online:

http://www.sensorsportal.com/HTML/BOOKSTORE/Digital_Sensors.htm



www.sensorsportal.com